

Magnetism of triangular nanoflakes with different compositions and edge terminations

Shunhong Zhang · Jian Zhou · Xiaowei Li · Qian Wang

Received: 28 October 2011 / Accepted: 28 August 2012
© Springer Science+Business Media B.V. 2012

Abstract Since the discovery of the giant magneto-resistance effect, extensive research has been devoted to finding new materials for spintronic devices. The hotly pursued nanostructure-based magnetic materials are potential candidates for such applications. Among them, graphene triangular nanoflakes (G-TNFs), due to their special magnetic configurations, can serve as building blocks for design of new C-based magnetic materials. This motivates the present study to systematically investigate how magnetism of the TNFs changes with their edge termination, composition, and atomic distribution. Using density functional theory, we show that the F-terminated G-TNFs have similar magnetic behavior to the H-terminated G-TNFs. Besides the edge terminations, partially hydrogenation of interior C atoms in the G-TNFs breaks the conjugate π orbitals and thus leads to extra net magnetic moment. The IV-group binary SiC-TNFs resemble the G-TNFs in magnetic properties, while the III-V group binary BN- and AlN-TNFs are different although they also have honeycomb structures. The different magnetic behaviors originate from

the different occupations of p_z atomic orbitals and the resulting change of conjugate π molecular orbitals. This study provides physical insight on tuning the magnetic behavior of TNFs through controlling their composition, size, and edge termination.

Keywords Nanoflakes · First-principles calculation · Electronic structure · Magnetism

Introduction

Nanostructures, due to their reduced size, low coordination, low dimensionality, and large surface to volume ratio, possess unique properties that are very different from their bulk. The ability to control the size, shape, and composition of nanostructures has created unprecedented possibilities to synthesize new materials with tailored functions. Among the extensively studied nanostructures such as nanoclusters, nanoparticles, fullerenes, nanocones, nanotubes, and nanowires, nanoflakes currently have attracted a considerable attention. A well-known example is graphene triangular nanoflakes (G-TNFs), which have been fabricated in experiments using chemical synthesis (Inoue et al. 2001), etching graphene sheet with electron beams (Jin et al. 2009; Chuvilin et al. 2009) and “nanocutting” (Ci et al. 2008). Compared to graphene nanoribbons (GNRs) and carbon chains, zigzag-edged G-TNFs have additional advantages in

S. Zhang · X. Li · Q. Wang (✉)
Center for Applied Physics and Technology, College
of Engineering, Peking University, Beijing 100871, China
e-mail: qianwang2@pku.edu.cn

J. Zhou
Department of Materials Science and Engineering,
College of Engineering, Peking University,
Beijing 100871, China

magnetic behavior (Fernandez-Rossier et al. 2007; Ezawa 2007, 2009; Şahin et al. 2010; Yazyev 2010; Philpott et al. 2010; Silva et al. 2010). It has been found that the magnetic coupling across the two zigzag edges of GNRs is antiferromagnetic (AFM) due to the anti-pattern rule in the sublattices A and B (Lee et al. 2005; Rudberg et al. 2007; Yamashiro et al. 2003), resulting in zero net magnetic moment. A finite C chain with even (bare ends) or odd (hydrogenated ends) number of carbon atoms only has a total magnetic moment of $2.0 \mu_B$ regardless of its length (Cahangirov et al. 2010; Li et al. 2009; Fan et al. 2009). However, in zigzag-edged G-TNFs, the spin alignments on their three edges couple ferromagnetically (Fernandez-Rossier and Palacios 2007; Ezawa 2007; Şahin et al. 2010; Yazyev 2010; Ezawa 2009). The total magnetic moment obeys Lieb's theorem (1989), and can be tuned by changing the size of TNFs. More importantly, magnetism in the G-TNFs, unlike that in conventional magnetic materials where magnetism is due to d or f electrons, originates from p electrons, displaying weak spin-orbit and hyperfine couplings which are the main channels of relaxation and decoherence of electron spins. These novel properties make G-TNFs promising as building blocks for new magnetic materials for transport of spin-polarized currents as well as for spin-based quantum information processing.

Recent theoretical studies show that the electronic and magnetic properties of G-TNFs can be changed significantly upon the termination of their edges (Şahin et al. 2010) or substitutional doping (Sheng et al. 2010). For example, the different magnetic moment values of $4(n-1)$, $(n-1)$, and $2(n-1) \mu_B$ were found for bare, singly, and doubly hydrogenated G-TNFs (Şahin et al. 2010), respectively, where n denotes the number of hexagons along each edge of the G-TNF. This result implies that the magnetic moment can be tuned not only by changing the size n but also by varying edge hydrogenation. Thus, questions arise: (1) How do the electronic and magnetic properties change with the edge termination and size n if some other elements, like fluorine, take the place of hydrogen? (2) Besides graphene sheet, currently, BN sheet and BN-C hybrid sheet have been synthesized (Han et al. 2008; Zhi et al. 2009; Ci et al. 2010; Wei et al. 2011), and existence and stability of SiC sheet and AlN sheet have been theoretically predicted (Freeman et al. 2006; Şahin et al. 2009). All

these atomic sheets have very similar geometries with graphene sheet, namely having the planar honeycomb structure and consisting of the two inequivalent sublattices A and B. Their zigzag-edged TNFs could be fabricated by etching these atomic sheets with electron beams. Are these TNFs also magnetic? How do the size and edge termination affect their electronic and magnetic properties? A fundamental understanding of these TNFs is crucial for the development of new materials for spintronics devices. In this paper, we have performed extensive studies on the TNFs with different size, edge termination, composition, and atomic distribution.

Computational method

Our calculations are based on spin-polarized density function theory (DFT) as implemented in the Dmol³ package (Delley 1990, 2000), which has been well tested and widely used in the studies of bulk and nanostructures. DFT is an efficient way to treat many-electron systems based on Hohenberg-Kohn theorem (Hohenberg and Kohn 1964) and Kohn-Sham equation (Kohn and Sham 1965). In calculations, we have used effective core potential with double-numerical plus polarization (DNP) basis set, which includes a p electron polarization function on hydrogen atoms, and have used generalized gradient approximation (GGA) for exchange-correlation potential given by Perdew et al. (1996). All the structures are relaxed without any symmetric constraints. The criteria of convergence of energy, force, and displacement are set to be 1×10^{-5} Ha, 0.002 Ha/Å, and 0.005 Å, respectively. The accuracy of our calculation procedure was tested by comparing our calculated results of H-terminated G-TNFs with previous work (Şahin et al. 2010). Our calculated equilibrium geometries, magnetic moments, and spin density iso-surfaces are found to be in agreement with those obtained by the other authors, e.g., for singly H-terminated G-TNF, the calculated magnetic moment and energy gap are $3 \mu_B$ and 0.67 eV, respectively, which are in good agreement with the values of $3 \mu_B$ and 0.64 eV (Şahin et al. 2010).

In this study, the size of a zigzag-edged TNF is defined by the number (n) of hexagons along one edge of the TNF, denoted by TNF _{n} . In general, a zigzag-edged G-TNF _{n} contains $(n^2 + 4n + 1)$ C atoms at the two inequivalent sublattice sites A and B. The edge

sites are defined as the A sites, and their neighboring sites are defined as B sites. Then, alternately, the B neighboring sites are the A sites. Therefore, the number of C atoms at the sublattice A sites is, $N_A = (n^2 + 5n)/2$. While that at the B sites is, $N_B = (n^2 + 3n + 2)/2$. We have explored three different ways to tune the magnetic properties of the TNFs, including edge termination, partially hydrogenation, and substitutional doping.

Results and discussion

Pristine G-TNFs with different edge terminations

We first study the effects of edge termination on the geometric, electronic, and magnetic properties of zigzag-edged G-TNFs, as magnetism of the G-TNFs comes mainly from their edge states. We consider the zigzag-edged G-TNF_n with size *n* from 3 to 7 and different edge terminations, namely singly and doubly H-terminations, respectively. Geometry optimization and the total energy calculations were carried out for all the configurations. It is found that the single H-termination does not change the planar honeycomb structure of the G-TNF_n. While the doubly H-saturated G-TNF_n exhibits visual buckling. The vertex C atoms are pulled out of the plane due to the edge atoms having *sp*³ hybridization. We quantify the distortion of a TNF_n by calculating the average deviation of the vertex C atoms from their positions in the un-relaxed planer structure in the normal direction of the TNF_n, which is 0.45 and 0.71 Å for the doubly H-terminated G-TNF_ns for *n* = 3 and 7 as examples, respectively. The distortion can be vanished when the G-TNFs are linked by some magnetic linkers to form periodic networks (Zhou et al. 2011, Li and Wang 2012). The spin density iso-surface of the G-TNF₄ with the single and double H-terminations are given in Fig. 1 a, b, and their corresponding energy spectra and spin-resolved density of states (DOS) near the Fermi level are plotted in Fig. 2 a, b, respectively, which show that spin polarization originates from the unpaired *p*_z electrons of the C atoms. In the singly H-terminated G-TNF₄, the predominant contribution to spin density comes from the edge C atoms. While it is significantly reduced in the doubly H-terminated G-TNF₄, their edge C atoms are in *sp*³ hybridization and have no unpaired electrons. In the doubly H-terminated G-TNFs, the spin polarization

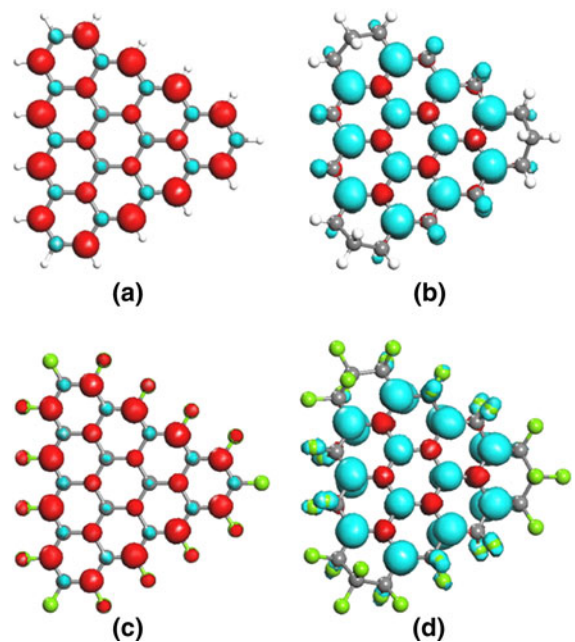


Fig. 1 Spin density iso-surface (with the value of 0.03 of $e\text{\AA}^{-3}$) of **a** singly and **b** doubly H-terminated G-TNF₄, and **c** singly and **d** doubly F-terminated G-TNF₄ flakes

mainly lies on the C atoms at the sublattice B sites. From the energy spectra (Fig. 2), we see that the energy levels, spin splitting, and the energy gap between the highest occupied molecular orbital (HOMO) and the lowest unoccupied molecular orbital (LUMO) change with the edge terminations. From the DOS, we see that the majority-spin (spin up for singly terminated G-TNF and spin down for doubly terminated G-TNF) channel generates a gap while the minority-spin channel spans across the Fermi level, which implies potential application in spin-filtering. The ratio (*R*) of the edge atoms to the total atoms is $R = 3n/(N_A + N_B) = 3n/(n^2 + 4n + 1)$. As the size *n* increases, *R* decreases, namely the edge effect becomes weaker as the size gets larger. Accordingly, the HOMO–LUMO gap reduces when the size increases, which can be expected to become zero when the size reaches the extreme case of infinite 2-D graphene. The change of HOMO–LUMO gap with respect to the size and edge termination is plotted in Fig. 3a. We see that the double H-termination is more effective than the single H-termination in tuning the energy gap.

The total magnetic moment of the G-TNF_ns (*n* = 3–7) with different H-terminations are calculated and listed in Table 1. It is found that the G-TNF_n with

Fig. 2 Energy spectra and DOS near the Fermi level of the G-TNF₄ with the different edge terminations. In the energy spectra and DOS, the HOMO energy is shifted to 0.00 eV, and the solid (dash) red and blue lines represent occupied (empty) spin up and down energy states, respectively

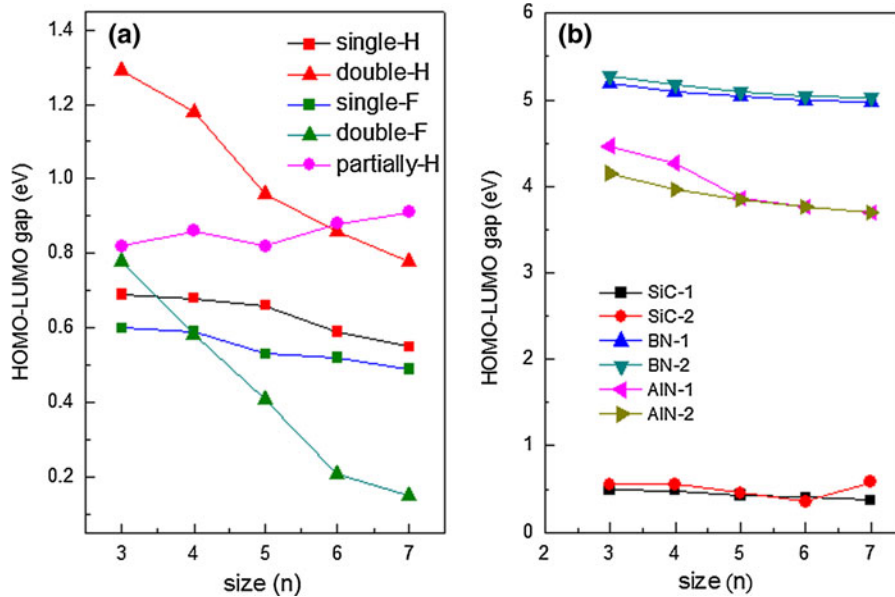
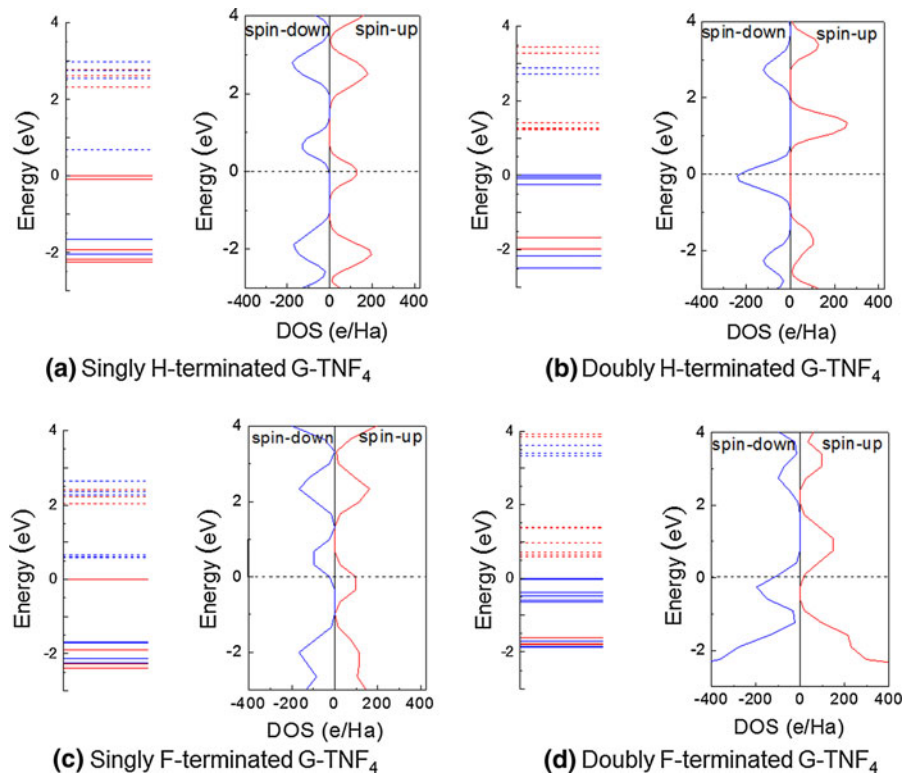


Fig. 3 Change of HOMO–LUMO gap with respect to size n of the G-TNF _{n} ($n = 3-7$) with different edge terminations and partially hydrogenation (a), and of the singly H-terminated binary compound TNF _{n} ($n = 3-7$) (b)

single or double H-termination has a total magnetic moment of $(n - 1)$ or $2(n - 1) \mu_B$, respectively. This is because in the singly H-terminated TNF _{n} s, all the C

atoms are in sp^2 bonding, similar to those in graphene. The difference of the number of C atoms at the sublattices A and B is: $(N_A - N_B) = (n - 1)$.

Table 1 Magnetic moment (in μ_B) of G-TNF_{*n*s} (*n* = 3–7) with different decorations and some typical BN and C hybridized TNF_{*n*s}

Size <i>n</i>	Singly-H/F	Doubly-H/F	Partially-H	BN@G-TNF NB@G-TNF	G@BN-TNF G@NB-TNF	Sierpinski-type BN@C-TNF
3	2.0	4.0	3.0			3.0
4	3.0	6.0	6.0	3.0	3.0	
5	4.0	8.0	10.0	3.0	4.0	6.0
6	5.0	10.0	15.0	3.0	5.0	
7	6.0	12.0	21.0	3.0	6.0	9.0

Therefore, the total moment is $(n - 1) \mu_B$. For a doubly H-terminated G-TNF_{*n*s}, the edge C atoms change to sp^3 hybridization, which have no contribution to the magnetic moment. Accordingly, the total moment is: $|(N_B - 3) - (N_A - 3n)| \mu_B = 2(n - 1) \mu_B$, where 3 and 3*n* are the numbers of edge C atoms at the sublattice sites B and A, respectively. Our calculated geometric, electronic, and magnetic properties of the G-TNFs with the H-terminations are in good agreement with previous work (Şahin et al. 2010).

We then replaced the H atoms with F to study the effect of edge fluorination on the electronic and magnetic properties of the G-TNFs, as similar to H atom, F also has one unpaired *p* electron. Following the same procedure as discussed above for the H-terminated G-TNFs, the calculations are carried out for the F-terminated G-TNF_{*n*s} with *n* = 3–7. It was found, for the singly F-terminated G-TNF_{*n*s}, the honeycomb planer structure is still kept. While the doubly F-termination results in small buckling. The distortion of G-TNF₃ and G-TNF₇ with their edge atoms doubly F-terminated is found to be 0.38 and 0.14 Å, respectively, which is much smaller than that in the H-terminated cases. All the F-terminated G-TNFs are also found to be spin-polarized, no matter whether their edges are singly or doubly F-terminated. The spin density iso-surface of the singly and doubly F-terminated G-TNF₄ are plotted in Fig. 1c, d, respectively, and their corresponding energy spectra and DOS near the Fermi level are plotted in Fig. 2c, d, respectively. They show that the spin polarization mainly comes from the unpaired p_z electrons of the C atoms, and the edge C atoms contribute more to spin density than the inner C atoms in the singly F-terminated G-TNF₄. In the doubly F-terminated systems, however, spin density on the edge C atoms is significantly reduced due to the sp^3 hybridization. Similar to that in the doubly H-terminated systems,

spin density mainly locates on the C atoms at the sublattice B sites.

The calculated magnetic moments are also tabulated in Table 1. It is interesting to see that the Lieb’s theorem (Lieb 1989) still holds and the size dependence of magnetism is the same as that of H-terminated G-TNF_{*n*s}, namely, the total moments of $(n - 1)$ and $2(n - 1) \mu_B$ are found for the singly and doubly F-terminated G-TNF_{*n*s}, respectively, although their bonding features are different due to the difference in electronegativity between H and F atoms. Covalent bonding is dominant in the H-terminations, while the partial ionic character is stronger in the F terminations due to the higher electron affinity of F atom. However, the two systems also share some similarities, namely, both of them have convent σ bonds, which lie far below the Fermi level. Their frontier orbitals are mainly contributed by π bonds (p_z electrons of C atoms). Since magnetism comes mainly from p_z electrons, therefore, H- and F-terminated G-TNFs show similar magnetic behaviors. In addition, the change of HOMO–LUMO gap with respect to its size is incorporated in Fig. 3a for comparison. We see that the double H- or F-termination of edge states is more effective in tuning the energy gap than the single termination, and the F-termination is more effective than the H-termination.

Partially hydrogenated G-TNFs

It has been found that hydrogenation is an effective way to tune graphene sheet from metallic to semiconducting and from nonmagnetic to magnetic. Theoretical study (Zhou et al. 2009) suggests that semi-hydrogenation breaks the delocalized π bonding network of graphene, leaving the p_z electrons in the un-hydrogenated carbon atoms localized and unpaired. Thus each sp^2 hybridized C atom carries 1 μ_B magnetic moment. The magnetic C

atoms couple ferromagnetically with each other through superexchange interactions via the hydrogenated C atoms. The theoretical prediction has been confirmed by recent experiments (Balog et al. 2010; Xie et al. 2011; Subrahmanyam et al. 2011). It would be interesting and important to know how the magnetic moment of a hydrogenated G-TNF changes with its size. Here, we take the G-TNF_{*n*} (*n* = 3–7) with their edges singly H-terminated as examples, and only consider a simple case where each C atom at the central B sites is hydrogenated as shown in Fig. 4a₁, b₁. We keep the C atoms in edge B sites un-hydrogenated so as to avoid huge distortion and keep the stability of the structure. Therefore, the difference between the C atoms at all the A sites and the un-hydrogenated C atoms at the edge B sites is $N_A - 3n = n(n - 1)/2$, which determines the total magnetic moment of the partially hydrogenated G-TNF_{*n*}. This is because each *p_z* orbital of the un-hydrogenated C atoms possesses a spin-polarized electron, similar to that in the infinite semi-hydrogenated graphene (Zhou et al. 2009). The magnetic C atoms at the edge A sites favor to couple antiferromagnetically with their nearest neighbor magnetic C atoms at the edge B sites, leading to the total moment of $n(n - 1)/2 \mu_B$ for the partially hydrogenated G-TNF_{*n*}. This is confirmed by our calculations, as given in Table 1. Spin densities of the partially hydrogenated G-TNF_{*n*} (*n* = 4, 5) are also plotted in Fig. 4a₂, b₂. We see that spin polarization emerges on the H sites, due to different electronegativity of C and H. When all the central A sites are hydrogenated and all the central B sites un-hydrogenated, the total moment turns to $N_B - 3n = (n - 1)(n - 2)/2$. Therefore, the magnetic moment is no longer a linear function of size *n* for the hydrogenated G-TNF_{*n*}, indicating that the hydrogenation is more efficient in tuning the magnetic moment.

The optimized geometries of the partially hydrogenated G-TNF_{*n*} are nonplanar as the hydrogenated C atoms have *sp*³ hybridization, which elongates the C–C bond length varying from 1.39 to 1.51 Å, comparable to that infinite semi-hydrogenated graphene sheet (1.495 Å) (Zhou et al. 2009). The percentage of hydrogenated C atoms is $x = (N_B - 3n)/(N_A + N_B) = (n^2 - 3n + 2)/(n^2 + 4n + 1)$. As *n* increases, *x* approaches to 50 % which is the limit of a two-dimensional sheet (Zhou et al. 2009). The HOMO–LUMO gap is in the range of 0.82–0.91 eV, and slightly oscillates with the size *n*, as shown in Fig. 3a. For the edge-terminated TNFs, the HOMO–LUMO gap

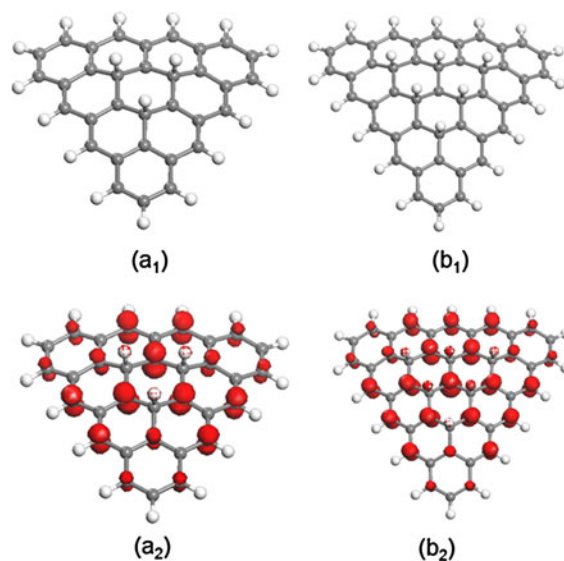


Fig. 4 a₁ and b₁ Optimized geometrical structures of partially hydrogenated G-TNF_{*n*} (*n* = 4 and 5); a₂ and b₂ their corresponding spin density iso-surfaces (0.12 e^{−3}), respectively

decreases with the increase of size. This is because as the size increases, the TNF gradually approaches to 2D graphene, accordingly the gap reduces. While for the partially hydrogenated TNFs, the HOMO–LUMO gap variation behavior is governed by the following two competing factors: As the size increases, the effect of quantum confinement is reduced, the HOMO–LUMO gap tends to decrease; On the other hand, larger partially hydrogenated TNFs have higher percentage of *sp*³ carbon atoms, which enhances the gap.

Binary compound TNFs

The well-known example of graphene-like binary compound one-atom-thick sheet is BN. Using a chemical-solution-derived method starting from singly-crystalline hexagonal BN, BN mono-atomic layer has been successfully synthesized (Han et al. 2008). Recently, an efficient method to fabricate high-yield 2D BN sheets has been developed by using a sonication–centrifugation technique (Zhi et al. 2009) where milligram quantity of BN sheets are achievable and ultimately pure BN sheets can be obtained based on a highly pure precursor. The triangular nanoflakes of BN have also been fabricated very recently (Xu et al. 2007), which have similar geometry to the G-TNFs. Thus, an interesting question arises: How are

the magnetic properties of BN sheet-based triangular nanoflakes (labeled as BN-TNFs) different from those of the G-TNFs? Here, we focus on the electronic and magnetic properties of zigzag-edged BN-TNFs. We start with the pure BN-TNFs without any edge termination. Different from the G-TNFs, there are two options for the edge atoms, i.e., either B or N. This leads to two chemical-unbalanced configurations: the B-edged and the N-edged BN-TNF_{*n*}, which have 3*n* edge B and N atoms located at sublattice A sites and 3 vertex N and B atoms located at sublattice B sites, respectively. Each edge (vertex) B atom has one unpaired electron, while each vertex (edge) N atom has a dangling bond as well as an unpaired electron. We carried out the calculations for the bare BN-TNF_{*n*}s with *n* = 4, 5, and 6. It was found that the optimized structures of all B-edged BN-TNF_{*n*}s (*n* = 4–6) nearly retain their initial planar structures, while some visible buckling is observed in the bare N-edge BN-TNF_{*n*}s. Their average distortion is in the range of 0.00–1.39 Å. Figure 5a₁, b₁ show that the two kinds of BN-TNFs exhibit different in-plan vertex deformation configurations. This is understandable because the relatively electron-rich N atoms near the vertexes tend to be repulsive to each other. The local spin polarization, however, is mainly on the edge and vertex atoms in both the B- and N-edged BN-TNF_{*n*}s, and all the edge atoms couple ferromagnetically, as shown in Fig. 5a₂, b₂. The total magnetic moment is calculated to be 3(*n* – 1) μ_B for both the B- and N-edged BN-TNF_{*n*}s. The amount is equal to the difference of unpaired electrons at the sublattice A and B sites. While the total magnetic moment is found to be 0.00 μ_B and all the systems become nonmagnetic, if their edges of the B- and N-edged BN-TNF_{*n*}s are singly H- or F-terminated. The geometries of all singly H- and F-terminated systems are kept well in the 2D planar structures. This is because the unpaired electrons of the edge and vertex atoms are paired due to the forming of the B(N)–H or B(N)–F bonds. The disappearance of spin polarization in these H- and F-terminated systems is the evidence of magnetism originating from unpaired electrons in their corresponding bare BN-TNFs.

Among the binary atomic sheets, AlN and SiC are other two examples. The both have been predicted to be stable with the 2D hexagonal geometry (Freeman et al. 2006; Şahin et al. 2009). The AlN and BN belong to the same III–V group, they have similar bonding

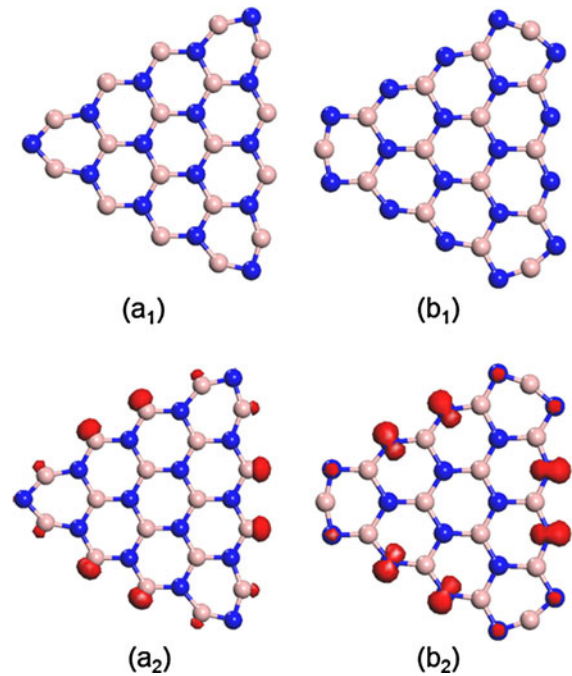


Fig. 5 Optimized geometrical structures of the B-edged (**a₁**) and N-edged BN-TNF₄ (**b₁**); and **a₂** and **b₂** their corresponding spin density iso-surfaces (0.25 eÅ⁻³), respectively

feature, namely, the B–N and Al–N bonds are more ionic-like than the C–C bonding, charge transfer results in the empty or filled *p_z* states in the B/Al or N sites. The strong electronegativity of N atoms makes electron-pairs localized in the N sites hence being unable to form delocalized π bonds like that in the G-TNF. We have indeed found that the AlN-TNF_{*n*}s (*n* = 4, 5, and 6) share similar features with the BN-TNF_{*n*}s, but the AlN-TNF_{*n*}s have larger geometrical distortions because Al is more metallic than B.

Similar to graphene, SiC sheet is a IV-group system, covalent binding is dominant. The *p_z* states can be expected to contribute and modulate the magnetism. We found that the SiC-TNF_{*n*}s exhibit quite similar magnetic behavior to the G-TNF_{*n*}s when their edges are singly terminated with H or F atoms, namely the moment varies with size *n* as (*n* – 1) μ_B. As examples, Fig. 6a₁, b₁ show the optimized geometries of the Si- and C-edged SiC-TNF₄ with single H-termination. All the SiC-TNF₄s remain the planar honeycomb structures well. The average Si–C bond length is 1.78 Å, which is in between 1.45 (for the BN) and 1.85 Å (for the AlN), and comparable with that in their corresponding infinite monolayer honeycomb

structure (Şahin et al. 2009). In Fig. 6a₂, b₂, the spin density distribution suggests that the edge states play an important role in magnetism of the SiC-TNFs, similar to the C-edges in G-TNFs.

In order to study the effect of edge species (Si or C, B or N) on the electronic structures of the above-mentioned SiC and BN binary systems, we plotted the HOMO and LUMOs in Fig. 7. For the SiC-TNF₄ systems, the HOMO and LUMO orbitals are doubly and triply degenerated, respectively. Magnetic orbitals are located around the Fermi level of the systems. We find that for the Si-edged SiC-TNF₄ (Fig. 7a), the HOMO and LUMO orbitals are contributed by the edged Si atoms, while in C-edged SiC-TNF₄, the edged C atoms contributed HOMO and LUMO orbitals (Fig. 7b). For the BN-TNF₄s, the HOMO and LUMO orbitals are quadruply and doubly degenerated, respectively. The HOMO orbitals are mainly contributed by the N atoms, and the LUMO orbitals mainly by the B atoms, similar to two-dimensional BN sheet (Zhou et al. 2010). Furthermore, the HOMO orbitals of N-edged BN-TNF₄ are more delocalized on all N atoms as compared to the LUMO orbitals.

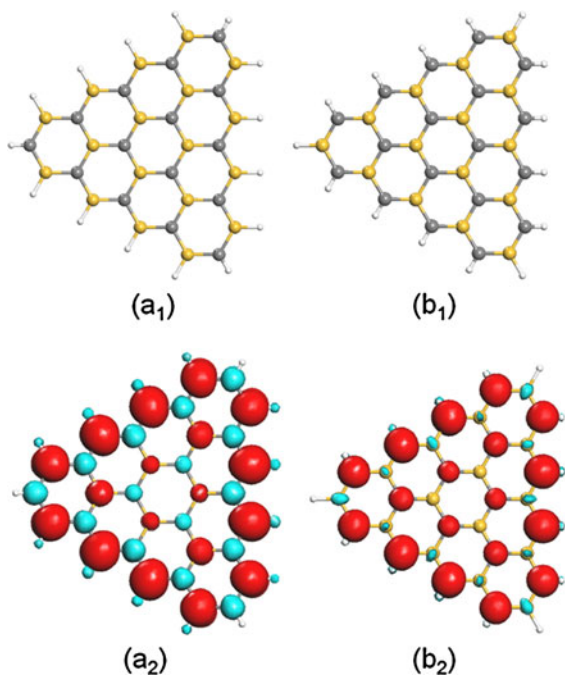


Fig. 6 Optimized geometrical structures of the Si-edged SiC-TNF₄ (**a**₁) and the C-edge SiC-TNF₄ (**b**₁); **a**₂ and **b**₂ their corresponding spin density iso-surfaces ($0.008 \text{ e}\text{\AA}^{-3}$), respectively

The situation is different for B-edged BN-TNF₄, where the LUMO orbitals are localized on the edge B atoms, while the HOMO orbitals are slightly delocalized. The HOMO–LUMO gap variations with respect to the size of single H-terminated binary TNFs are plotted in Fig. 3b. We can conclude that for the binary TNF systems, the edge atoms can affect the frontier orbital distributions significantly.

BN-C hybridized TNFs

B, C, and N are neighbors in the periodic table. In geometry, their similarities exist between C₆H₆ and B₃N₃H₆, as well as graphene and BN sheet, respectively. The physical and chemical properties of carbon and its BN counterpart, however, are quite different. For example, C₆H₆ is aromatic, while B₃N₃H₆ is non-aromatic. Graphene sheet is metallic-like, while BN sheet is a wide-gap semiconductor. The similarities and dissimilarities have stimulated a considerable interest in C–BN hybrid structures, as the similarity in their geometries guarantees the match in lattice and bond length, while the dissimilarity in their properties provides the diversity and tunability of their functions and performance. In fact, BN–C hybrid nano-sheet (Ci et al. 2010; Wei et al. 2011), nanotube (Wei et al. 2011) and nanoribbons (Wei et al. 2011) have been theoretically studied and experimentally synthesized. Controllable C substitutional doping in BN nanostructures has also been achieved via in situ electron beam irradiation (Wei et al. 2011). Based on the hybrid BN–C sheets or nanoribbons, hybrid BN@C-TNFs could be fabricated by using electron beam irradiation and etching techniques. Here, we take $n = 5$ as an example to study how magnetism changes with the distribution of BN and C atoms in the hybrid TNFs. We consider two kinds of hybrid structures, namely a BN-TNF embedded in the G-TNF₅ or a G-TNF embedded in the BN-TNF₅. For each of them, there are two options when BN binds with C: either through N or B atoms (Liu et al. 2011). Therefore, the four configurations are generated, as shown in Fig. 8a–d, and labeled as BN@G-TNF₅, NB@G-TNF₅, G@BN-TNF₅, and G@NB-TNF₅. The Sierpinski-type hybrid structures are also taken into account, as plotted in Fig. 8e, f. Their corresponding spin distributions are calculated and also plotted in Fig. 8. We see the common features: the main contributions to magnetism are from the C atoms, which weakly polarize

Fig. 7 Frontier orbitals at the iso-value of $0.03 \text{ e}\text{\AA}^{-3}$ for the Si-edged SiC-TNF₄ (a), the C-edged SiC-TNF₄ (b), the N-edged BN-TNF₄ (c), and the B-edged BN-TNF₄ (d). The numbers in brackets refer to energy degeneracy

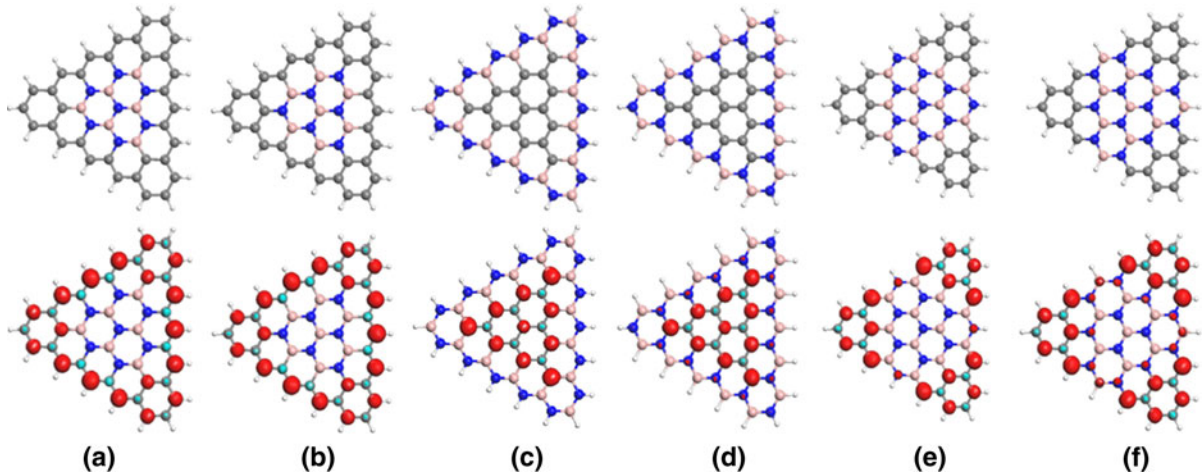
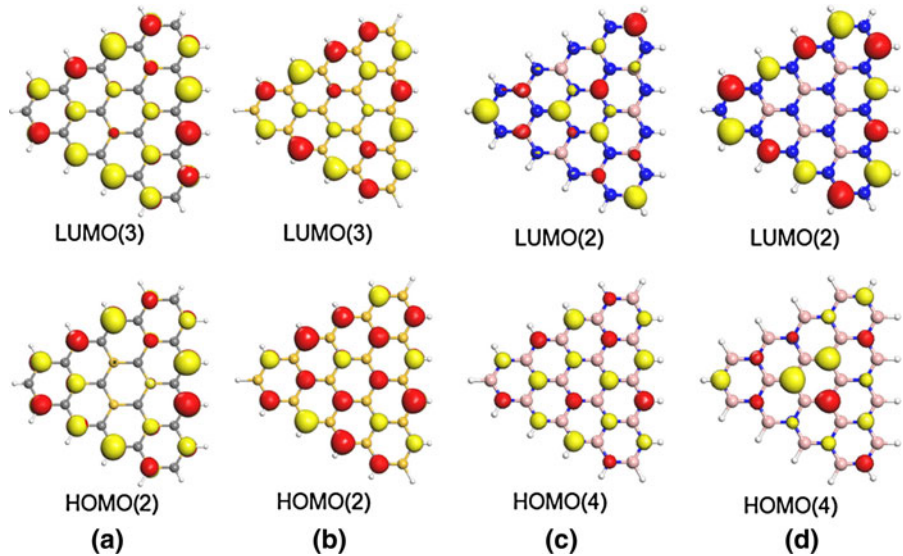


Fig. 8 Geometry (*up panel*) and spin density (*bottom panel*) of BN@G-TNF₅ (a), NB@G-TNF₅ (b), G@BN-TNF₅ (c), G@NB-TNF₅ (d), and Sierpinski-type hybrid structures (e, f). The iso-surfaces of spin density are set at the iso-value of $0.05 \text{ e}\text{\AA}^{-3}$

their neighboring atoms. While the N atoms are more polarizable when compared to the B atoms because they are electron-rich. These features can also be seen in the hybrid Sierpinski-type structures (Fig. 8, e, f).

It is interesting to see that the total magnetic moment of the hybrid TNFs depends on the pattern (distribution of atoms). For example, in Fig. 8a, b the three zigzag edge chains are composed of C atoms, and there is a C atom (labeled as C_{vertex}) on each of the three corners connecting with the BN patch. We found that this kind of hybrid TNFs have a total

magnetic moment of $3 \mu_B$, independent of the size. This is because the difference between the C atoms at the sublattices A and B is a constant number of 3. While, if the three C_{vertex} atoms are replaced by three N or B atoms, the total moment diminishes to zero. When a G-TNF patch is embedded in the BN-TNF₅ and NB-TNF₅ with the configurations as shown in Fig. 8c, d, respectively, the change of total magnetic moment with respect to the size n of the hybrid TNFs follows $(n - 1)$ which is the difference of sublattices of A and B. While, the magnetic moment of Sierpinski-type BN@C-TNFs is found to be

$\frac{3}{2}(n-1)\mu_B$ when n is odd numbers. The calculated results are summarized in Table 1.

Conclusion

In summary, extensive calculations were carried out to understand the magnetic properties of TNFs with different sizes, compositions, and edge terminations. The following conclusions can be drawn: (1) The G-TNF_{*n*} with F-terminations results in similar magnetic behavior to the H-terminated G-TNF_{*n*}, namely the total magnetic moment is a linear function of size n and it changes from $(n-1)$ to $2(n-1)$ when going from single to double fluorinations. (2) The linear behaviors are changed when the G-TNF_{*n*} is partially hydrogenated, which varies as $n(n-1)/2$ for the studied configurations; when all the B sites are kept un-hydrogenated and all the central A sites are hydrogenated, the total moment changes as $(n-1)(n-2)/2$. (3) For the III–V binary systems like the BN-TNFs and AlN-TNFs, because of the charge transfer, the p_z states are either empty or filled, exhibiting very different behaviors from the G-TNFs. In both the B- and N-edged BN-TNF_{*n*}s, the total magnetic moment is $3(n-1)\mu_B$ with all the edge atoms couple ferromagnetically. All the systems, however, become nonmagnetic when the B- and N-edged BN-TNF_{*n*} being singly H- or F-terminated. While for the IV binary system like the SiC-TNFs, due to the covalent bonding between Si and C, the p_z states and the total magnetic moment display similar behaviors to that in the G-TNFs. (4) Since graphene and BN sheets have very good match in geometry and bond length, the 2D planar structures are kept in their hybrid TNFs. Magnetism of the hybridized TNFs can be delicately tuned by changing their atomic configurations, although it is dominated by the C atoms. The present study suggests that the existence of unpaired p_z electrons plays a crucial role in magnetism of the TNFs, providing physical insight into the origin of magnetism in the new TNFs.

Acknowledgments This work is partially supported by grants from the National Natural Science Foundation of China (Grant Nos. NSFC-11174014 and NSFC-21273012), and the National Grand Fundamental Research 973 Program of China (Grant No. 2012CB921404).

References

- Balog R, Jørgensen B, Nilsson L, Andersen M, Rienks E, Bianchi M, Fanetti M, Lægsgaard E, Baraldi A, Lizzit S, Slijivancanin Z, Besenbacher F, Hammer B, Pedersen TG, Hofmann P, Hornekær L (2010) Bandgap opening in graphene induced by patterned hydrogen adsorption. *Nat Mater* 9:315–319
- Cahangirov S, Topsakal M, Ciraci S (2010) Long-range interactions in carbon atomic chains. *Phys Rev B* 82:195444–195448
- Chuvilin A, Meyer JC, Algara-Siller G, Kaiser U (2009) From graphene constrictions to singly carbon chains. *New J Phys* 11:083019–083029
- Ci L, Xu Z, Wang L, Gao W, Ding F, Kelly KF, Yakobson BI (2008) Controlled nanocutting of graphene. *Nano Res* 1:116–122
- Ci L, Song L, Jin C, Jariwala D, Wu D, Li Y, Srivastava A, Wang ZF, Storr K, Balicas L, Liu F, Ajayan PM (2010) Atomic layers of hybridized boron nitride and graphene domains. *Nat Mater* 9:430–435
- Delley B (1990) An all-electron numerical method for solving the local density functional for polyatomic molecules. *J Chem Phys* 92:508–517
- Delley B (2000) From molecules to solids with the DMol3 approach. *J Chem Phys* 113:7756–7764
- Ezawa M (2007) Metallic graphene nanodisks: electronic and magnetic properties. *Phys Rev B* 76:245415–245420
- Ezawa M (2009) Quasiphase transition and many-spin Kondo effects in a graphene nanodisk. *Phys Rev B* 79:241407–241410(R)
- Fan XF, Liu L, Lin JY, Shen ZX, Kuo J (2009) Density functional theory study of finite carbon chains. *ACS Nano* 3:3788–3794
- Fernandez-Rossier J, Palacios JJ (2007) Magnetism in graphene nanoislands. *Phys Rev Lett* 99:177204–177207
- Freeman CL, Claeysens F, Allan NL, Harding JH (2006) Graphitic nanofilms as precursors to wurtzite films: theory. *Phys Rev Lett* 96:066102–066105
- Han WQ, Wu L, Zhu Y, Watanabe K, Taniguchi T (2008) Structure of chemically derived mono- and few-atomic-layer boron nitride sheets. *Appl Phys Lett* 93:223103–223105
- Hohenberg P, Kohn W (1964) Inhomogeneous electron gas. *Phys Rev* 136:864–871
- Inoue J, Fukui K, Kubo T, Nakazawa S, Sato K, Shiomi D, Morita Y, Yamamoto K, Takui T, Nakasuji K (2001) The first detection of a clar's hydrocarbon, 2,6,10-tri-tert-butyl-triangulene: a ground-state triplet of non-kekulé polynuclear benzenoid hydrocarbon. *J Am Chem Soc* 123:12702–12703
- Jin C, Lan H, Peng L, Suenaga K, Iijima S (2009) Deriving carbon atomic chains from graphene. *Phys Rev Lett* 102:205501–205504
- Kohn W, Sham LJ (1965) Self-consistent equations including exchange and correlation effects. *Phys Rev* 140:1133–1138
- Lee H, Son Y, Park N, Han S, Yu J (2005) Magnetic ordering at the edges of graphitic fragments: magnetic tail interactions between the edge-localized states. *Phys Rev B* 72:174431–174438
- Li XW, Wang Q (2012) Tunable ferromagnetism in assembled two dimensional triangular graphene nanoflakes. *Phys Chem Chem Phys* 14:2065–2069
- Li ZY, Sheng W, Ning ZY, Zhang ZH, Yang ZQ, Guo H (2009) Magnetism and spin-polarized transport in carbon atomic wires. *Phys Rev B* 80:115429–115433

Balog R, Jørgensen B, Nilsson L, Andersen M, Rienks E, Bianchi M, Fanetti M, Lægsgaard E, Baraldi A, Lizzit S,

- Lieb EH (1989) Two theorems on the Hubbard model. *Phys Rev Lett* 62:1201–1204
- Liu Y, Bhowmick S, Yakobson BI (2011) BN white graphene with “colorful” edges: the energies and morphology. *Nano Lett* 11:3113–3116
- Perdew J, Burke K, Ernzerhof M (1996) Generalized gradient approximation made simple. *Phys Rev Lett* 77:3865–3868
- Philpott MR, Vukovic S, Kawazoe Y, Lester WA Jr (2010) Edge versus interior in the chemical bonding and magnetism of zigzag edged triangular graphene molecules. *J Chem Phys* 133:044708–044715
- Rudberg E, Sałek P, Luo Y (2007) Nonlocal exchange interaction removes half-metallicity in graphene nanoribbons. *Nano Lett* 7:2211–2213
- Şahin H, Cahangirov S, Topsakal M, Bekaroglu E, Akturk E, Senger RT, Ciraci S (2009) Monolayer honeycomb structures of group-IV elements and III-V binary compounds: first-principles calculations. *Phys Rev B* 80:155453–155464
- Şahin H, Senger RT, Ciraci S (2010) Spintronic properties of zigzag-edged triangular graphene flakes. *J Appl Phys* 108:074301–074305
- Sheng W, Ning ZY, Yang ZQ, Guo H (2010) Magnetism and perfect spin filtering effect in graphene nanoflakes. *Nanotechnology* 21:385201–385207
- Silva AM, Pires MS, Freire VN, Albuquerque EL, Azevedo DL, Caetano EWS (2010) Graphene nanoflakes: thermal stability, infrared signatures, and potential applications in the field of spintronics and optical nanodevices. *J Phys Chem C* 114:17472–17485
- Subrahmanyam KS, Kumar P, Maitra U, Govindaraj A, Hembram KPSS, Waghmare UV, Rao CNR (2011) Chemical storage of hydrogen in few-layer graphene. *Proc Natl Acad Sci USA* 108:2674–2677
- Wei X, Wang M, Bando Y, Golberg D (2011) Electron-beam-induced substitutional carbon doping of boron nitride nanosheets, nanoribbons, and nanotubes. *ACS Nano* 5:2916–2922
- Xie L, Wang X, Lu J, Ni Z, Luo Z, Mao H, Wang R, Wang Y, Huang H, Qi D, Liu R, Yu T, Shen Z, Wu T, Peng H, Özyilmaz B, Loh K, Wee ATS, Ariando Chen W (2011) Room temperature ferromagnetism in partially hydrogenated epitaxial graphene. *Appl Phys Lett* 98:193113–193115
- Xu L, Zhan J, Hu J, Bando Y, Yuan X, Sekiguchi T, Mitome M, Golberg D (2007) High-yield synthesis of rhombohedral boron nitride triangular nanoplates. *Adv Mater* 19:2141–2144
- Yamashiro A, Shimoi Y, Harigaya K, Wakabayashi K (2003) Spin- and charge-polarized states in nanographene ribbons with zigzag edges. *Phys Rev B* 68:193410–193413
- Yazyev OV (2010) Emergence of magnetism in graphene materials and nanostructures. *Rep Prog Phys* 73:056501–056516
- Zhi C, Bando Y, Tang C, Kuwahara H, Golberg D (2009) Large-scale fabrication of boron nitride nanosheets and their utilization in polymeric composites with improved thermal and mechanical properties. *Adv Mater* 21:2889–2893
- Zhou J, Wang Q, Sun Q, Chen XS, Kawazoe Y, Jena P (2009) Ferromagnetism in semihydrogenated graphene sheet. *Nano Lett* 9:3867–3870
- Zhou J, Wang Q, Sun Q, Jena P (2010) Electronic and magnetic properties of a BN sheet decorated with hydrogen and fluorine. *Phys Rev B* 81:085442–085448
- Zhou J, Wang Q, Sun Q, Jena P (2011) Intrinsic ferromagnetism in two-dimensional carbon structures: triangular graphene nanoflakes linked by carbon chains. *Phys Rev B (Rapid Commun)* 84:081402–081405(R)